Highly stable two-dimensional silicon phosphides: Different stoichiometries and exotic electronic properties

Bing Huang, Houlong L. Zhuang, Mina Yoon, Bobby G. Sumpter, and Su-Huai Wei

Phys. Rev. B **91**, 121401 — Published 3 March 2015

DOI: 10.1103/PhysRevB.91.121401

Highly Stable Two-dimensional Silicon Phosphides: Different Stoichiometries and Exotic Electronic Properties

Bing Huang, Houlong L. Zhuang, Mina Yoon, and Bobby G. Sumpter

Oak Ridge National Laboratory, Oak Ridge, TN 37830, USA

Su-Huai Wei

National Renewable Energy Laboratory, Golden, CO 80401, USA

(Dated: February 13, 2015)

Abstract

The discovery of stable two-dimensional, earth-abundant, semiconducting materials is of great interest and may impact future electronic technologies. By combining global structural prediction and first-principles calculations, we have theoretically discovered several previously unknown semiconducting silicon phosphide (Si_xP_y) monolayers, which could be formed stably at the stoichiometries of y/x≥1. Interestingly, some of these compounds, i.e., P-6m2 Si_1P_1 and Pm Si_1P_2, have comparable or even lower formation enthalpies than their previously known allotropes. The band gaps (E_g) of Si_xP_y compounds can be dramatically tuned in an extremely wide range ($0< E_g < 3$ eV) by simply changing the number of layers. Moreover, we find that carrier doping can drive the ground state of C2/m Si_1P_3 from a nonmagnetic state into a robust half-metallic spin-polarized state, originating from its unique valence band structure, which can extend the use of Si-related compounds for spintronics.

The successful exfoliation of monolayer graphene opened a rapid growing research direction in condensed matter physics, that is, two-dimensional (2D) materials. In the past few years, tremendous interest has begun to focus on the search for novel 2D semiconducting materials beyond graphene. For example, 2D transition-metal dichalcogenides that have been achieved experimentally by chemical or mechanical methods[1] show interesting valley-dependent electronic properties[2] and an indirect-direct band gap transition as a function of the number of layers[1, 3]. Earth-abundant silicon and phosphorus-related compounds are extremely important for electronic and optoelectronic applications, such as transistors and solid-state lighting[4]. Very recently, silicene (monolayer silicon)[5–7] and phosphorene (monolayer black phosphorus)[8–10] have been successfully achieved in several experiments. Both silicene and phosphorene have a graphenelike honeycomb lattice but with different surface puckered structures. While silicene can only be stabilized on metal substrates[5–7], phosphorene is stable after exfoliation and could be a promising candidate for transistor applications[8–10].

The currently known earth-abundant semiconducting 2D materials are still very limited, and it is therefore highly desired to discover more of these types of materials to satisfy various electronic applications. Usually, alloying can be used to broadening or go beyond material properties of their constituent parents for specific applications. For examples, (In,Ga)N alloys are critical solid-state lighting materials for different colors[11] and Cu(In,Ga)Se_2 alloys are one of three mainstream thin-film photovoltaic materials in the current market[12]. While 2D Si and P have been achieved in recent experiments, an interesting question is whether stable 2D silicon phosphide (Si_xP_y) monolayers with different stoichiometries can exist in the Si-P phase diagram? If so, what kind of stable stoichiometries can they have, and do they have more attractive electronic properties than that of 2D Si and P? The answers to these questions are not only scientifically important to extend our current knowledge of 2D materials, but also can provide a promising approach for the discovery of new 2D functional materials beyond the existing materials.

By combining global structural search and first-principles calculations, we have theoretically found several novel stable or metastable semiconducting Si_xP_y monolayers, which can only be formed at the stoichiometries of $y/x \geq 1$. Interestingly, the predicted P-6m2 Si_1P_1 and Pm Si_1P_2 monolayers have similar or even lower formation enthalpies (ΔH) than their previously known bulk allotropes. The band gaps (E_g) of Si_xP_y compounds can be tuned in

a very wide range by simply changing the number of layers. Furthermore, we find that hole doping can convert the ground state of C2/m Si_1P_3 from a nonmagnetic state to a robust ferromagnetic (half-metallic) state, originating from its unique valence band structure.

To find the stable 2D Si_xP_y compounds that have not been observed in experiments, we have conducted an unbiased structure search based on particle swarm optimization (PSO), as implemented in the CALYPSO code[13]. We focus on the different stoichiometries as Si/P ratios ranging from 3:1 (Si_3P_1) to 1:3 (Si_1P_3). For PSO predictions, any combination of numbers of atoms in the unit cell are allowed (with the total number $\leq$18 atoms). First-principles density functional theory (DFT) methods, as implemented in the VASP package[14], are used for structural relaxation and electronic structure calculations. The projector augmented wave method in conjunction with the generalized gradient approximation within the framework of Perdew-Burke-Ernzerhof is adopted for the electron exchange and correlation. The kinetic energy cutoff for the plane wave basis is set to 400 eV. A slab containing 20 Å vacuum region in the normal direction is selected to simulate isolated 2D materials. Sufficient Γ-centered k-point mesh is carried out over the Brillouin zone for all the structures, ensuring approximately the same k-point density among different-sized supercells. All the structures are fully relaxed until the force on each atom is less than 0.01 eV/Å. It is well known that DFT underestimates the E_g of semiconductors, therefore, we have also performed accurate GW self-energy calculations[15, 16] for several selected systems. To ensure the dynamical stability of our predicted structures, we use the finite displacement method, as implemented in PHONOPY code[17], to calculate the phonon frequencies.

Figure 1 summarizes the calculated formation enthalpies ΔH of various 2D Si_xP_y at different P compositions. ΔH is defined as $\Delta H = H(Si_xP_y) - xH_{Si} - yH_P$ and all the ΔH in Figure 1 are given per atom at zero temperature. Thermodynamically, a Si_xP_y phase is stable or metastable against decomposition to elements if its ΔH value is negative. Diamond silicon and bulk black phosphorus, which are known to be the most stable phases of Si and P, are selected to calculate the element enthalpies of Si (H_{Si}) and P (H_P), respectively. When x/y>1 (Si-rich condition), we cannot find any stable 2D Si_xP_y phases with negative ΔH values. The lowest-ΔH phases for x/y=3 and x/y=2 are C2/m Si_3P_1 and P-1 Si_2P_1[16], respectively. Their ΔH values are significantly positive, i.e., 0.145 eV/atom for C2/m Si_3P_1 and 0.127 eV/atom for P-1 Si_2P_1.

Interestingly, when $y/x \geq 1$, a large number of Si_xP_y monolayers with negative ΔH emerge

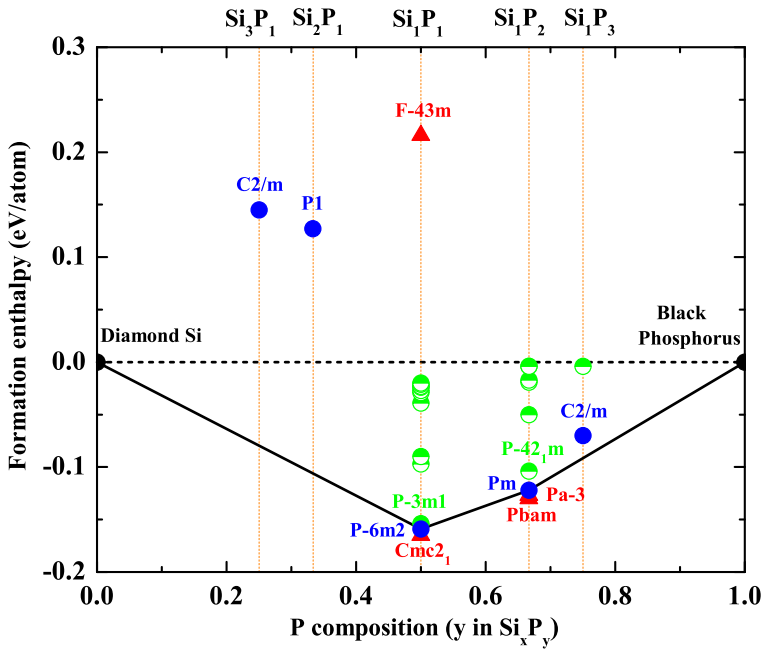

FIG. 1: Thermodynamic stability of 2D Si_xP_y indicated by the calculated formation enthalpies (ΔH) of various 2D Si_xP_y compounds with respect to elemental decomposition into diamond silicon and black phosphorus. The solid-blue circles represent the predicted lowest-ΔH Si_xP_y at each P composition. The half-filled-green circles represent other predicted Si_xP_y compounds with negative ΔH values. The ground-state convex hull of 2D Si-P compounds is denoted by the solid lines. For comparison, the calculated ΔH values of four previously known bulk Si_xP_y compounds, i.e., F-43m Si_1P_1, $Cmc2_1$ Si_1P_1, Pbam Si_1P_2, and Pa-3 Si_1P_2, are also plotted as red triangles.

and most of these satisfy the classical electron counting rule, i.e., Si atoms are fourfold coordinated while P atoms are threefold coordinated to realize full sp^3 hybridization. For the stoichiometry of Si_1P_1, the lowest-ΔH phase has a GaSe-type (hexagonal, P-6m2) structure with ΔH=-0.159 eV/atom, as shown in Fig. 2a. P-3m1 phase (Fig. 2b), which shares a similar structure with P-6m2 phase but with inversion symmetry, has a negligibly higher ΔH value (5 meV/atom) than that of P-6m2 phase. Except for P-3m1 and P-6m2 phases, there are nine metastable Si_1P_1 allotropes with negative ΔH values, and five compounds among them have similar structural characteristics[16]. We show one typical example in Fig. 2c, which has $P2_1/m$ symmetry. In these five structures, the zigzag SiP chain (top view in Fig. 2c) is the basic building block to produce these structures. The different arrangements (numbers and orientations) of these SiP chains give rise to these five low-ΔH Si_1P_1 phases.

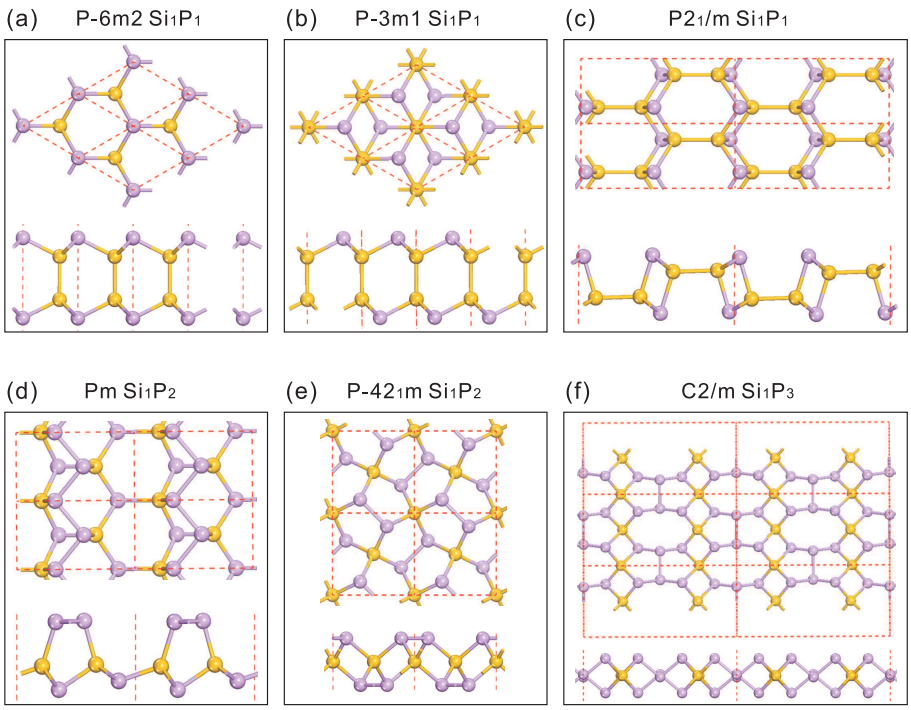

FIG. 2: Structures of 2D Si_xP_y. The top view (upper) and side view (lower) of (a) P-6m2 Si_1P_1, (b) P-3m1 Si_1P_1, (c) $P2_1/m$ Si_1P_1, (d) Pm Si_1P_2, (e) P-42_1m Si_1P_2, and (f) C2/m Si_1P_3. Violet and yellow spheres are P and Si atoms, respectively. The unit cells are marked by the red dashed lines.

When the P composition is further increased to the stoichiometry of Si_1P_2, seven Si_1P_2 with negative ΔH values appear in the phase diagram. The lowest-ΔH phase has Pm symmetry with ΔH=-0.122 eV/atom. As shown in Fig. 2d, the Pm Si_1P_2 structure can be considered as the stacking of one zigzag P chain on the *h*-BN-like SiP monolayer in each unit cell. The second lowest-ΔH phase is P-42_1m Si_1P_2, which has a slightly higher ΔH (17 meV/atom) than that of Pm phase. Interestingly, the Si_2P_3 pentagon is the basic building block to form the P-42_1m Si_1P_2 structure, as shown in Fig. 2e. Other negative-ΔH phases of Si_1P_2 are shown in Ref.[16]. For the stoichiometry of Si_1P_3, we find two structures with negative ΔH. And the lowest-ΔH (-0.069 eV/atom) one has C2/m symmetry, as shown in Fig. 2f. For a given stoichiometry of Si_xP_y, although there are several structures with similar ΔH, it is still possible to achieve a single crystalline Si_xP_y phase, because the diverse structural characteristics of different phases could give rise to large transition energy barriers.

The structural stabilities of these predicted structures were also checked by phonon spectrum calculations[16]. The phonon calculations demonstrate that these predicted 2D Si_xP_y

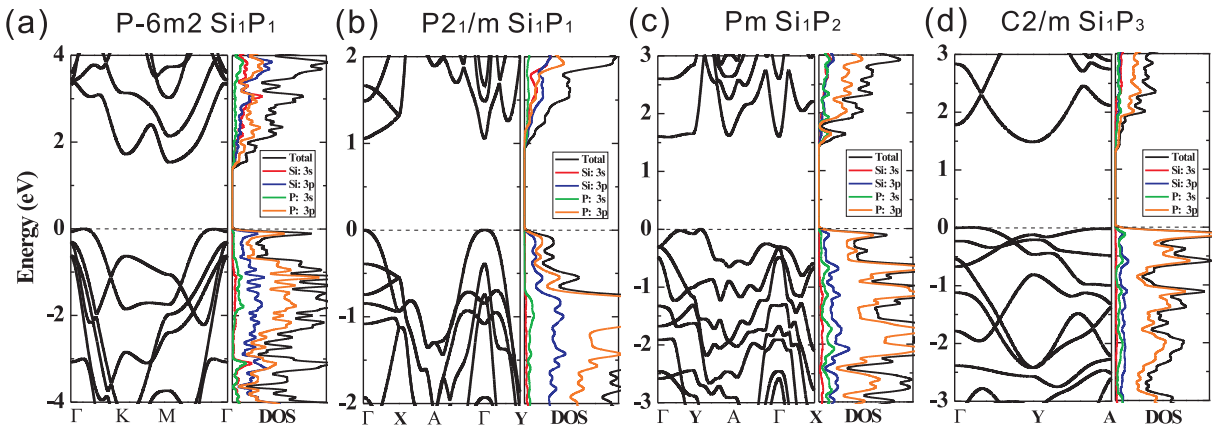

FIG. 3: Electronic structures of 2D Si_xP_y. The DFT-calculated band structures of (a) P-6ma Si_1P_1, (b) $P2_1/m$ Si_1P_1, (c) Pm Si_1P_2, and (d) C2/m Si_1P_3. The total and partial density of states (DOS) of these structures are also plotted in (a)-(d). The Fermi level is set to zero.

structures are dynamically stable without any imaginary phonon modes. Based on the calculated ΔH values of all the 2D Si_xP_y, we can obtain the ground-state convex hull of 2D Si_xP_y, as shown in Figure 1. Obviously, P-6m2 Si_1P_1 and Pm Si_1P_2 are located on the convex hull, indicating that they are stable against disproportioning into other neighboring compounds. In practice, the synthesis of P-6m2 Si_1P_1 monolayer could be similar to the chemical growth of monolayer GaSe[18]. It is also important to compare the thermal stabilities of our predicted monolayer Si_xP_y to the previously known existing bulk Si_xP_y phases. Four crystalline Si_xP_y phases were reported in past experiments[19–21] and their calculated ΔH are shown in Figure 1 (red triangles). For the stoichiometry of Si_1P_1, the bulk $Cmc2_1$ phase has a negligibly lower ΔH value (6 meV/atom) than our predicted monolayer P-6m2 phase, while the bulk F-43m phase has a significantly positive ΔH value of 0.216 eV/atom. For the stoichiometry of Si_1P_2, the predicted monolayer Pm phase also has a quite similar ΔH value (ΔH difference <10 meV/atom) as the bulk Pbam and Pa-3 phases. It is worth noticing that despite the energy difference between diamond and graphite being as large as ~20 meV/atom[22], both phases can stably exist in nature. Because our calculated ΔH differences are even smaller, we believe that (at least) the predicted P-6m2 (and P-3m1) Si_1P_1, Pm (and P-42_1m) Si_1P_2, and C2/m Si_1P_3 phases should be able to be formed as easily as their existing allotropes, at least under nonequilibrium growth conditions by carefully selecting specific substrates. They might also exist in nature but have not yet be discovered.

The DFT-calculated band structures of these 2D Si_xP_y compounds are shown in Figure 3. As shown in Fig. 3a, P-6m2 Si_1P_1 is an indirect gap semiconductor with E_g of 1.54 eV. The valence band maximum (VBM) is contributed by the hybridized *3p* (π) orbitals from P and Si atoms, while the conduction band minimum (CBM) is contributed by the hybridized *3s* and *3p* orbitals of Si and P atoms. Interestingly, we find that the valence band dispersion around Fermi level (E_F) in this structure is similar to that of GaSe[18, 23]. This unusual flat valence band dispersion around Γ-point and E_F gives rise to a rather high DOS and a van Hove singularity around the VBM. The more accurate GW-E_g of P-6m2 Si_1P_1 is 2.61 eV, and the band dispersion around E_F is close to that of DFT results[16]. The band structure of P-3m1 Si_1P_1 is similar to the P-6m2 one[16], and the DFT (GW) E_g is 1.78 (2.97) eV. Comparing to the calculated GW-E_g, we can estimate that the DFT-E_g of Si_xP_y monolayer is roughly underestimated by ∼1.1 eV. $P2_1/m$ Si_1P_1 is a direct gap semiconductor with a DFT-E_g of 1.05 eV at the Γ-point. Its VBM is contributed by the Si-P *3p* (σ) orbitals, while CBM is contributed by the Si *3p* (π) and *3s* orbitals (Fig. 3b). As shown in Fig. 3c, Pm Si_1P_2 is a (quasi)direct semiconductor with a DFT-E_g of 1.58 eV. Its VBM is mainly contributed by the P 3*p* states, while its CBM is mainly contributed by the P *3s* and *3p* orbitals. P-42_1m Si_1P_2 (Fig. 2e) is an indirect semiconductor with a DFT-E_g of 1.89 eV[16]. C2/m Si_1P_3 (Fig. 3d) is a weakly indirect gap semiconductor with a DFT-E_g of 1.49 eV. Its minimum direct gap (1.61 eV) is located at the Y-point. The VBM is mostly contributed by the P *3p* (π) state and CBM is mainly contributed by the hybridized P *3s* and *3p* orbitals. This unique atomic non-bonding-like character of P *3p* states around VBM results in an extremely high DOS and van Hove singularity. The DFT-E_g of other metastable Si_xP_y (with negative ΔH) are in a wide range of 0.49∼1.80 eV[16].

According to the Stoner criterion, spontaneous ferromagnetism could appear if the exchange splitting energy is larger than the loss in kinetic energy, i.e., if the DOS at E_F is high enough[24, 25]. Since P-6m2 Si_1P_1 (Fig. 3a) and C2/m Si_1P_3 (Fig. 3d) have very large DOS around the VBM, by doping holes into these two systems, one can shift the E_F to a position with high DOS so that it may satisfy the Stoner criterion. The spin polarization energy (E_p), defined by the energy difference between the spin-polarized state and nonspin-polarized state, was calculated to check the stability of spin-polarization. As expected, these two systems can indeed be converted into ferromagnetic ground state at critical hole densities (n_h), as shown in Fig. 4a. For P-6m2 Si_1P_1, the range of 0.20∼0.40μ_B/hole can be achieved when

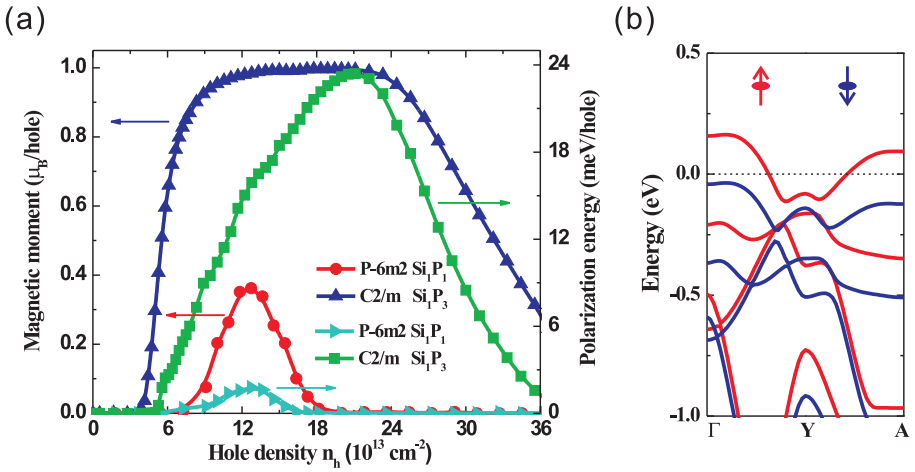

FIG. 4: Magnetic properties of 2D Si_xP_y. (a) The magnetic moments and spin-polarization energies of 2D P-6m2 Si_1P_1 and C2/m Si_1P_3 as a function of carrier (hole) density n_h. (b) The DFT-calculated (valence) band structure of C2/m Si_1P_3 at n_h=1.5×10^{14}cm^{-2}. The spin-up and spin-down bands are shown as red and blue colors, respectively. The Fermi level is set to zero.

1×10^{14}<n_h<1.6×10^{14}cm^{-2}. However, the maximum E_p of Si_1P_1 is ≤2 meV/hole, which means that an extremely low temperature is necessary to stabilize the spin-polarization. Interestingly, C2/m Si_1P_3 has a much stronger spin-polarization effect upon hole doping, which is consistent with the fact that the DOS around VBM in C2/m Si_1P_3 is about six times higher than that of P-6m2 Si_1P_1. As shown in Fig. 4a, the spin moment in Cm/2 Si_1P_3 is rapidly increasing when n_h>4×10^{13}cm^{-2}, as the DOS at E_F in the system is increasing. The system finally reaches a plateau of ∼1μ_B/hole when 8×10^{13}<n_h<2.5×10^{14}cm^{-2}. As an example, Fig. 4b shows the band structure of Si_1P_3 at n_h=1.5×10^{14}cm^{-2}. Here, the system now behaves as an ideal half-metallic phase, i.e., 100% spin-polarization around E_F. When n_h>2.5×10^{14}cm^{-2}, the spin moment gradually decreases, as the DOS at E_F decreases. Remarkably, we find that E_p could be significantly high (>10 meV/hole) in a wide range of n_h (8×10^{13}<n_h<3×10^{14}cm^{-2}), indicating that the ferromagnetic states are very stable, which is important for practical applications. This is also the first prediction that half-metallicity could be achieved in 2D Si-/P-based compounds. It is worth noting that high carrier densities have already been experimentally achieved in other monolayer materials by applying gate voltages, such as graphene (4×10^{14}cm^{-2})[26] and MoS_2 (2×10^{14}cm^{-2})[27].

It is also interesting to understand the thickness effects on the electronic properties of these 2D Si_xP_y. We select P-6m2 Si_1P_1 as an example to study the E_g as a function of the

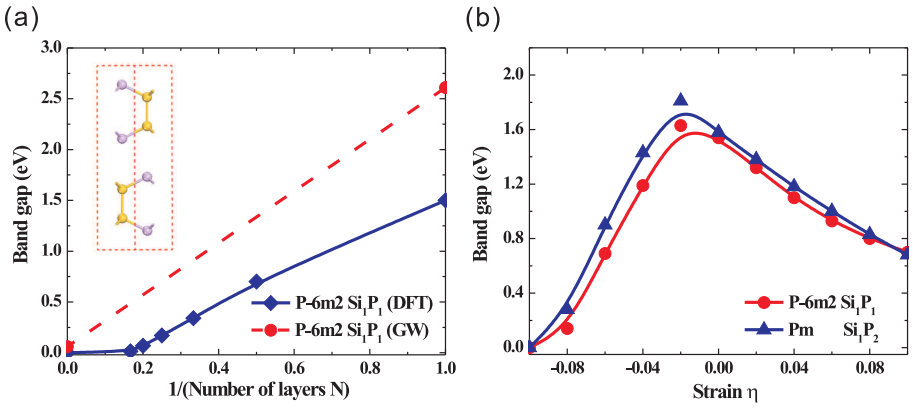

FIG. 5: Thickness and strain dependent electronic properties of 2D Si_xP_y. (a) The DFT and GW calculated band gaps of P-6m2 Si_1P_1 as a function of the number of layers. The dashed lines connect the band gaps corrected by GW calculation. Inset: the side view of the structure of bulk β-Si_1P_1. (b) The DFT calculated band gaps of P-6m2 Si_1P_1 and Pm Si_1P_2 monolayer as a function of in-plane strain η.

number of layers (N). Just as for GaSe[28], Si_1P_1 layers can form four different bulk crystal structures, i.e., β-, ϵ-, γ-, and δ-Si_1P_1. The β-stacking ($P6_3/mmc$, inset of Fig. 5a) has a negligibly lower energy than other stacking types[29]. Surprisingly, as N increases, DFT-E_g is dramatically decreased from 1.54 eV (monolayer) to 0 eV (negative E_g). The more accurate GW calculations also confirm that the E_g of bulk β-Si_1P_1 is $\sim$0 eV[16]. Importantly, our calculations also demonstrate that this N-dependent metal-insulator transition is very robust and generally exists in the ϵ-, γ-, and δ-stacking Si_1P_1 systems. The N-dependent E_g is much more noticeable than that in MoS_2 and GaSe[1, 3, 18], which could be attractive for the applications where metal-insulator transition is desired.

Finally, we find that an in-plane strain η can also dramatically change E_g and even its characters from direct (indirect) to indirect (direct) in 2D Si_xP_y, similar to the pure phosphorene layers[8, 30]. For example, a large η can significantly reduce the E_g of monolayer Si_1P_1 and Si_1P_2 (Fig. 5b). Especially, when η<-2%, Si_1P_2 is converted from a direct gap semiconductor to an indirect one, which could be very useful for optical applications.

In conclusion, we have theoretically identified several previously unknown stable or metastable semiconducting Si_xP_y monolayers. As the new family members of 2D materials, these Si_xP_y monolayers not only have significantly different structures compared to their constituent parents, but also show very unusual and promising electronic (e.g., metal-

insulator transition) and magnetic (e.g., half-metallicity) properties beyond their constituent parents. More generally, our study provides an experimentally achievable idea to discover new functional 2D materials, via alloying, for broader electronic applications.

The work at ORNL was supported by the Scientific User Facilities Division (BGS, MY) and the Materials Science and Engineering Division (BH, HLZ), Basic Energy Sciences, U.S. Department of Energy. The research at NREL (SHW) was sponsored by the U.S. Department of Energy under Contract No. DE-AC36-08GO28308. Computing resources provided by the Leadership Computing Facility at Oak Ridge National Laboratory and National Energy Research Scientific Computing Center, which is supported by the Office of Science of the U.S. Department of Energy under Contract No. DE-AC02-05CH11231.

[1] Q. H. Wang, K. Kalantar-Zadeh, A. Kis, J. N. Coleman, and M. S. Strano, Nature Nano. **7**, 699 (2012).

[2] X. Xu, W. Yao, D. Xiao, and T. F. Heinz, Nature Phys. **10**, 343 (2014).

[3] K. F. Mak, C. Lee, J. Hone, J. Shan, and T. F. Heinz, Phys. Rev. Lett. **105**, 136805 (2010).

[4] M. Peruzzini and Luca Gonsalvi, *Phosphorus Compounds: Advanced Tools in Catalysis and Material Sciences*, Springer (2011).

[5] P. Vogt, P. De Padova, C. Quaresima, J. Avila, E. Frantzeskakis, M. C. Asensio, A. Resta, B. Ealet, and G. L. Lay, Phys. Rev. Lett. **108**, 155501 (2012).

[6] L. Chen, C. Liu, B. Feng, X. He, P. Cheng, Z. Ding, S. Meng, Y. Yao, and K. Wu, Phys. Rev. Lett. **109**, 056804 (2012).

[7] A. Fleurence, R. Friedlein, T. Ozaki, H. Kawai, Y. Wang, Y. Yamada-Takamura, Phys. Rev. Lett. **108**, 245501 (2012).

[8] H. Liu, A. T. Neal, Z. Zhu, Z. Luo, X. Xu, D. Tomanek, and P. D. Ye, ACS Nano **8**, 4033 (2014).

[9] S. P. Koenig, R. A. Doganov, H. Schmidt, A. H. Castro Neto, and B. Ozyilmaz, Appl. Phys. Lett. **104**, 103106 (2014).

[10] L. Li, Y. Yu, G. J. Ye, Q. Ge, X. Ou, H. Wu, D. Feng, X. H. Chen, and Y. Zhang, Nature Nanotech. **9**, 373 (2014).

[11] A. Bergh, G. Craford, A. Duggal, and R. Haitz, Phys. Today **54**, 42 (2001).

[12] P. Jackson, D. Hariskos, E. Lotter, S. Paetel, R. Wuerz, R. Menner, W. Wischmann, and M. Powalla, Prog. Photovoltaics **19**, 894 (2011).

[13] Y. Wang, J. Lv, L. Zhu, and Y. Ma, Phys. Rev. B **82**, 094116 (2010).

[14] G. Kresse and J. Furthmüller, Comput. Mater. Sci. **6**, 15 (1996).

[15] M. Hybertsen and S. G. Louie, Phys. Rev. B **34**, 5390 (1986); L. Wirtz, A. Marini, and A. Rubio, Phys. Rev. Lett. **96**, 126104 (2006); C. -H. Park, C. D. Spataru, and S. G. Louie, Phys. Rev. Lett. **96**, 126105 (2006).

[16] See Supplementary Material for additional information regarding other metastable Si_xP_y, GW calculation methods and results, phonon spectrums of Si_xP_y, electronic structures of Si_xP_y as a function of strain or thickness.

[17] A. Togo, F. Oba, and I. Tanaka, Phys. Rev. B **78**, 134106 (2008).

[18] X. Li, W. Lin, A. Puretzky, J. C. Idrobo, C. Ma, M. Chi, M. Yoon, C. M. Rouleau, I. I. Kravchenko, D. B. Geohegan, and K. Xiao, Sci. Rep. **4**, 5497 (2014).

[19] J. Osugi, R. Namikawa, and Y. Tanaka, Rev. Phys. Chem. Jap. **36**, 35 (1966).

[20] P. C. Donohue, W. J. Siemons, and J. L. Gillson, J. Phys. Chem. Solids **29**, 807 (1968).

[21] T. Wadsten, Chem. Commun. **7**, 1 (1973).

[22] P. Hawtin, J. B. Lewis, M. Moul, and R. H. Philips, Philos. Trans. R. Soc. London, Ser. A **261**, 67 (1966).

[23] V. Zolyomi, N. D. Drummond, and V. I. Falko, Phys. Rev. B **87**, 195403 (2013).

[24] B. Huang, F. Liu, J. Wu, B. -L. Gu, and W. H. Duan, Phys. Rev. B **77**, 153411 (2008).

[25] H. Peng, H. J. Xiang, S. -H. Wei, S. -S. Li, J. Xia, and J. Li, Phys. Rev. Lett. **102**, 017201 (2009).

[26] D. K. Efetov and P. Kim, Phys. Rev. Lett. **105**, 256805 (2010).

[27] J. T. Ye, Y. J. Zhang, R. Akashi, M. S. Bahramy, R. Arita, and Y. Iwasa, Science **338**, 1193 (2012).

[28] A. Kuhn, A. Chevy, and R. Chevalier, Phys. Stat. Sol. (a) **31**, 469 (1975).

[29] Van de Waals interactions are described using optB86-vdW functional [J. Klimes, D. R. Bowler, and A. Michaelides, Phys. Rev. B **83**, 195131 (2011)].

[30] Z. Zhu and D. Tománek, Phys. Rev. Lett. **112**, 176802 (2014); J. Guan, Z. Zhu, and D. Tománek, Phys. Rev. Lett. **113**, 046804 (2014).